



1 **Investigation of an extreme rainfall event during 8–12 December 2018 over central**
2 **Viet Nam – Part 2: An evaluation of predictability using a time-lagged cloud-resolving**
3 **ensemble system**

4 Chung-Chieh Wang¹, Duc Van Nguyen^{1,2}, Thang Van Vu², Pham Thi Thanh Nga², Pi-Yu
5 Chuang¹, and Kien Ba Truong^{2,*}

6 Correspondence: kien.cbg@gmail.com

7 ¹Department of Earth Sciences, National Taiwan Normal University, Taipei, Taiwan

8 ²Viet Nam Institute of Meteorology, Hydrology and Climate Change, Hanoi, Viet Nam

9 **Abstract:**

10 This is the second part of a two-part study that investigates an extreme rainfall event that
11 occurred from 8 to 12 December 2018 over central Viet Nam (referred to as the D18 event).
12 In this part, the study aims to evaluate the predictability of the D18 event using a time-
13 lagged cloud-resolving ensemble and a quantitative precipitation forecast system. To do
14 this study, 29 time-lagged (8 days in lead time) high resolution (2.5 km) members were
15 run, with the first members run at 12:00 UTC 3 December 2018, and the last member-run
16 at 12:00 UTC 10 December 2018. Between the first and the last members are multiple
17 members that run every 6-h. The evaluated results reveal that CReSS well predict the
18 rainfall fields at the short-range forecast (less than 3 days) for 10 December (rainiest day).
19 Particularly, results show CReSS has high skills in heavy-rainfall QPFs for the 24-h rainfall
20 of 10 Dec with the SSS scores greater than 0.5 for both the last five members and the last
21 nine members. These good results are due to the model having good predicts of other
22 meteorological variables, such as surface wind fields. However, these prediction skills are
23 reducing at extending lead time (longer than 3 days), and it is challenging to achieve the
24 prediction of QPF for rainfall thresholds greater than 100 mm with lead time longer than 6
25 days. Besides, the ensemble sensitivity analysis of 24-hour rainfall responds to the initial
26 conditions shows that the 24-hour rainfall is very sensitive with initial conditions, not only
27 at the lower level but also at the upper level. The ensemble-based sensitivity is decreased



28 with the increasing lead time. Through the analysis of thermodynamic and moisture
29 sensitivities, it showed that the features of ESA facilitated a better understanding of the
30 sensitivity of a precipitation forecast to the initial conditions, implying that it is meaningful
31 to apply ESA to control initial conditions by work in the future.

32 **1 Introduction**

33 The present study is the second part of a two-part study investigating the extreme rainfall
34 event during 8–12 December 2018 over central Viet Nam (referred to as the D18 event
35 hereafter). D18 event is a record-breaking rainfall event which occurred along the mid-
36 central coast, from Quang Binh to Quang Ngai provinces. The observational data shows
37 that particularly heavy rainfall with the maximum 3-days accumulated rainfall from 12:00
38 UTC on 8 December to 12:00 UTC on 11 December exceeding 800 mm (Fig. 1f). In which,
39 the rainiest day is 10 December with 24-h observed data exceed 600 mm at some stations
40 (Fig. 4 OBS). This record-breaking rainfall event led to 13 dead, many destructions in the
41 environment, downstream cities, and many other economic losses due to catastrophic
42 flooding and landslides. In part 1 ([Wang and Nguyen 2023](#)), we focused on the analysis of
43 the mechanism that caused this event and evaluated the simulation by the Cloud-Resolving
44 Storm Simulator ([CReSS; Tsuboki and Sakakibara, 2002, 2007](#)). The analyzed results
45 point out the main factors which led to this event as well as its spatial rainfall distribution.
46 These factors included the combined interaction between the strong northeasterly winds
47 and easterly winds over the South China Sea (SCS) in the lower troposphere (below 700
48 hPa). The local terrain also played essential role due to its barrier effect. The cloud model's
49 good simulation results in part 1 indicated its promising potential in forecasting this event.
50 Hence, in part 2, the present study focuses on an evaluation of its predictability of the D18
51 event through a series of time-lagged high resolution ensemble quantitative precipitation
52 forecasts (QPFs) by the CReSS model.

53 Until now, predicting heavy rainfall events is still challenging to meteorologists and
54 weather forecasters, although great progresses in both computer science and atmospheric
55 science have been made. The prediction of heavy to extreme rainfall is more difficult for



56 Viet Nam, where both multi-scale interactions among different weather systems and strong
57 influence by local topography often exist. For example, when D18 event occurred, several
58 operational models were unable to predict this event successfully. Specifically, Fig. 1
59 shows the predictions for the D18 event by three global models at the National Centers for
60 Environmental Prediction (NCEP), the European Centre for Medium-Range Weather
61 Forecasts (ECMWF), and the Japan Meteorological Agency (JMA), and by one mesoscale
62 regional model, the Weather Research and Forecasting (WRF) model, implemented for
63 operation at the Mid-central regional Hydro-Meteorological center in Da Nang city, Viet
64 Nam. While these models overall made good predictions in the surface wind field, their
65 72-h accumulated rainfall amounts along the coast of central Viet Nam (less than 250 mm)
66 were much lower than the observation, which exceeded 900 mm (Fig. 1). Therefore, in
67 order to improve the QPFs for heavy rainfall events in Viet Nam, we need to not only
68 understand their mechanisms of occurrence, but also develop better forecasting tools.

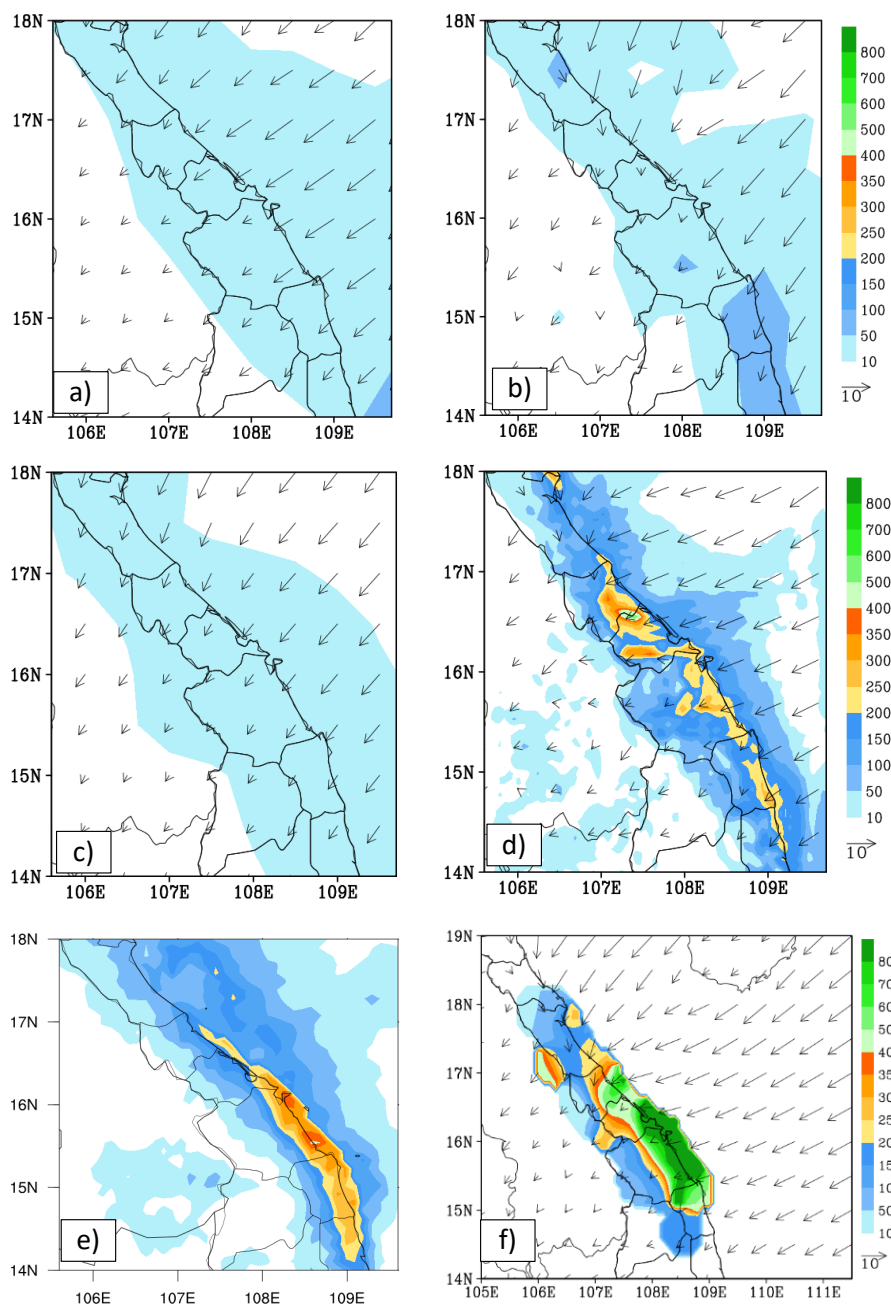
69

70

71

72

73



74

75 **Figure 1.** The predicted 72h accumulated rainfall (mm, shaded) and mean surface wind
76 (ms^{-1} , vector) for the period of 12:00 UTC 8 December – 12:00 UTC 11 December 2018



77 obtained by (a) NCEP, (b) ECMWF, (c) JMA, (d) WRF, (e) 72h accumulated rainfall
78 obtained by the Global Precipitation Measurement (GPM) estimate (IMERG Final Run
79 product) and (f) 72h observed accumulated rainfall (mm, shaded) and the mean surface
80 wind derived from ERA5 data (ms^{-1} , vector), adapted from Fig. 14c of [Wang and Nguyen](#)
81 [2023](#).

82 Among several different methods, the present-day weather forecasts depend mainly on
83 numerical weather prediction (NWP) using models, a scientific method that has become
84 indispensable for its ability to simulate weather and produce quantitative results (Fig. 1).
85 However, there is always uncertainty in the numerical forecasts due to the fact that the
86 atmosphere is a chaotic system and tiny errors in the initial state can grow rapidly and lead
87 to large errors in the forecast. Various approximations in numerical methods are also
88 sources of forecast uncertainty. Thus, by generating a range of possible weather conditions
89 in days ahead or into the future, the ensemble forecasting was introduced as an effective
90 method to estimate forecast uncertainty and improve the overall accuracy and usefulness
91 of NWP products. For example, some studies have shown high skill in QPFs for extreme
92 rainfall produced by typhoons in Taiwan using the CReSS model, a cloud-resolving model
93 (CRM), with high resolution and time-lagged approach ([Wang et al. 2016](#); [Wang 2015](#);
94 [Wang et al. 2014](#); [Wang et al. 2013](#)). Table 1 of [Wang et al. \(2016\)](#) shows that the high-
95 resolution time-lagged ensemble forecasts provide overall better quality in comparison
96 with both the traditional low-resolution ensemble forecasts and high-resolution
97 deterministic forecasts at a comparable cost in computation. Furthermore, some studies
98 show that the ensemble mean typically has smaller errors than individual members. This
99 error reduction is because the high predictability features that the members agree on are
100 emphasized by the mean, while the low-predictability ones that the members do not agree
101 on are filtered out or dampened (e.g., [Leith 1974](#); [Murphy 1988](#), [Surcel et al. 2014](#)).

102 Besides the advantages of ensemble forecasts described above, the ensemble-based
103 sensitivity analysis (ESA) also helps effectively investigate how sensitive the forecast
104 variables are and to what preceding factors. To be more specific, [Torn and Hakim \(2009\)](#)



105 used ESA to evaluate how their subject, tropical cyclones (TCs) undergoing extratropical
106 transition, in the prediction respond to a change in the initial condition. In their results, the
107 cyclone minimum sea-level pressure forecasts are determined as strongly sensitive to TC
108 intensity and position at short lead times and equally sensitive to mid-latitude troughs that
109 interacted with the TC at longer lead times. For an extreme rainfall event in northern
110 Taiwan, [Wang et al. \(2021\)](#) performed ESA using the results from 45 forecast members
111 with a grid size of 2.5–5 km to identify contributing factors to heavy rainfall. By
112 normalizing their impacts on rainfall using standard deviation (SD), different factors can
113 be compared quantitatively and on an equal footing. Ranked by their importance, these
114 factors included the position of the surface Mei-yu front and its moving speed (-16.00 mm
115 per 5 km h^{-1}), the position of 700-hPa wind shift line and its speed ($+12.59$ mm per 0.4°
116 latitude), the moisture amount in the environment near the front ($+11.73$ mm per 0.92 g
117 kg^{-1} in mixing ratio), timing and location of frontal mesoscale low-pressure disturbance
118 ($+11.03$ mm per 1.38° longitude), and (5) frontal intensity ($+9.58$ mm per 3 K in equivalent
119 potential temperature difference across 0.5°). Many other studies also used the ESA to
120 study TCs, convective events, or support the development of operational ensemble
121 sensitivity-based techniques to improve probabilistic forecasts ([Kerr et al. 2019](#), [Hu and](#)
122 [Wu 2020](#), [Coleman and Ancell 2020](#)).

123 For heavy precipitation over central Viet Nam, [Son and Tan \(2009\)](#) used the Mesoscale
124 Model version 5 (MM5) to investigate the predictability of heavy rainfall events over the
125 southern part of central Viet Nam during the period of 2005 and 2007. Their results showed
126 that MM5 can predict heavy rainfall there and its performance is better for events caused
127 by TCs or TC interactions with the cold air. [Toan et al. \(2018\)](#) assessed the predictability
128 of heavy rainfall events in middle-central Viet Nam due to combined effects of cold air and
129 easterly winds using the WRF model within a forecast range of 2 days. The evaluation
130 indicated that for 24-h lead time, the model performed reasonably well at rainfall thresholds
131 less than 100 mm day^{-1} . For 48-h forecast range, the model performed well only at
132 thresholds below 50 mm day^{-1} and had some skill at $50\text{--}100 \text{ mm day}^{-1}$. However, heavy



133 rainfall events at thresholds over 100 mm day⁻¹ were almost unpredictable by the model.
134 [Nhu et al. \(2017\)](#) also used the WRF model to investigate the role of the topography in
135 central Viet Nam on the occurrence of a heavy rainfall event there in November 1999. In
136 this study, the model well simulated the northeast monsoon circulation, TCs, and the
137 occurrence of heavy rainfall in central Viet Nam. Furthermore, when the topography is
138 removed, the three-day total accumulated rainfall decreased sharply (by approximately
139 75%) compared to that in the control experiment with the terrain. [Hoa Van Vo \(2016\)](#)
140 examined the predictability of heavy-rainfall events during the wet seasons of 2008–2012
141 in the middle section and central highlands of Viet Nam using NWP products from several
142 global models, including the Global Forecasting System (GFS) from NCEP, Global
143 Spectral Model (GSM) from JMA, Navy Operational Global Atmospheric Processing
144 System (NOGAPS) from the US Navy, and the Integrated Forecast System (IFS) from
145 ECMWF. Their results indicated that IFS and GSM performed better than GFS and
146 NOGAPS, and IFS was evaluated the best. However, all four global models under-
147 estimated rainfall in extreme events.

148 The review above suggests that considerable limitations still exist in forecasting heavy
149 rainfall in central Viet Nam, especially using coarser models. It also indicates that a high-
150 resolution time-lagged ensemble approach may offer some advantages in the prediction of
151 extreme rainfall events, such as a better simulation of local weather conditions, a quicker
152 response to changes in forecast uncertainty in real time, and potentially a longer lead time
153 for hazard preparation. Climatologically, the entire Viet Nam lies in the tropical zone (Fig.
154 2a), where vigorous but less organized convection often develops in response to local
155 conditions, while the region is also prone to the influence and interactions of weather
156 systems spanning a wide range of scales as reviewed. In addition, although central Viet
157 Nam is a small region with the narrowest place only about 80 km in width, it possesses
158 significant topography running in the north-south direction to affect rainfall (Fig. 2a).
159 Hence, a high-resolution CRM with detailed and explicit treatment in cloud microphysics
160 is likely crucial for better QPFs in central Viet Nam. Consequently, the present study used



161 the CReSS model to investigate the predictability of the D18 event through a series of time-
162 lagged ensemble predictions. The rest of this paper is organized as follows. Section 2
163 describes the data, model, and methodology used in the study. The model results are
164 presented and evaluated in Section 3. Finally, conclusions are offered in Section 4.

165 **2 Data and methodology**

166 2.1 Data

167 *2.1.1 The International Grand Global Ensemble retrieval*

168 The International Grand Global Ensemble (TIGGE) retrieval is a key component of The
169 Observing System Research and Predictability Experiment (THORPEX) research
170 program, whose aim is to accelerate the improvements in the accuracy of 1-day to 2-week
171 high-impact weather forecasts. The TIGGE retrieval provides not only deterministic
172 forecast data but also ensemble prediction datasets from major centers, including NCEP of
173 the USA, MetOffice of the United Kingdom (UKMO), ECMWF of the European Union,
174 and JMA of Japan, since 2006. This dataset has been used for a wide range of research
175 studies on predictability and dynamical processes. In this study, we used the global model
176 predictions to analyze the predictability of the D18 event. The variables utilized included
177 total precipitation and surface winds (u - and v -wind components at 10-m height) from
178 NCEP, ECMWF, and JMA at 6-h intervals during our data period (as shown in Figs. 1a-c)
179 from 12:00 UTC 8 to 12:00 UTC 11 December 2018 (as shown in Figs. 1a-c). The data
180 linked is placed in the “code and data availability” section.

181 *2.1.2 NCEP GFS historical archive*

182 In this study, the NCEP GFS data from the analyses and forecast runs executed every 6 h,
183 at 00:00, 06:00, 12:00, and 18:00 UTC daily, were used to drive the CReSS model
184 predictions. The horizontal resolution of the data is $0.25^\circ \times 0.25^\circ$, and 26 of vertical levels,
185 and the forecast fields are provided every 3 h from the initial time out to a range of 192 h.
186 The data linked is also placed in the “code and data availability” section.



187 *2.1.3 Observation data*

188 The daily observed rainfall data (12:00–12:00 UTC, i.e., 19:00–19:00 LST) from 8 to 12
189 December 2018 at 69 automated gauge stations across central Viet Nam is used for case
190 overview and verification of model results. This dataset is provided by the Mid-Central
191 Regional Hydro Meteorological Center, Viet Nam. The spatial distribution of these gauge
192 stations is depicted in figure 2b.

193 *2.1.4 The Global Precipitation Measurement (IMERG Final Run) data*

194 The Global Precipitation Measurement (GPM) is a mission international jointly by the
195 National Aeronautics and Space Administration (NASA) and the Japan Aerospace
196 Exploration Agency (JAXA), employing an international satellite network for advanced
197 global rain and snow observations. The GPM *IMERG Final Run* is a research-level product
198 which is created by intercalibrate, merging, and interpolating “all” satellite microwave
199 precipitation estimates, along with microwave-calibrated infrared (IR) satellite estimates,
200 analyses from precipitation gauges, and potentially other precipitation estimation
201 methodologies at fine time and space scales. The horizontal resolution of this dataset is 0.1°
202 $\times 0.1^\circ$ latitude–longitude and the time resolution is every 30 minute. In this study, we used
203 this satellite data to verify rainfall distribution over the coastal sea due to the limitation of
204 the observation station network, we only have the observation stations inland, as shown in
205 the Fig. 2b. This dataset was downloaded from 12:00 UTC on 8 December to 12:00 UTC
206 on 11 December 2018 to analyze the D18 event as well as the rainiest day of this event (10
207 December).

208 *2.1.5 The WRF data*

209 The WRF is implemented for operational numerical forecast system at Mid-central regional
210 Hydro- Meteorological center, Viet Nam. In this study, we used this data to analysis the
211 predictability of D18 event using the mesoscale numerical prediction. The download
212 variables include precipitation, the surface U wind component and surface V wind



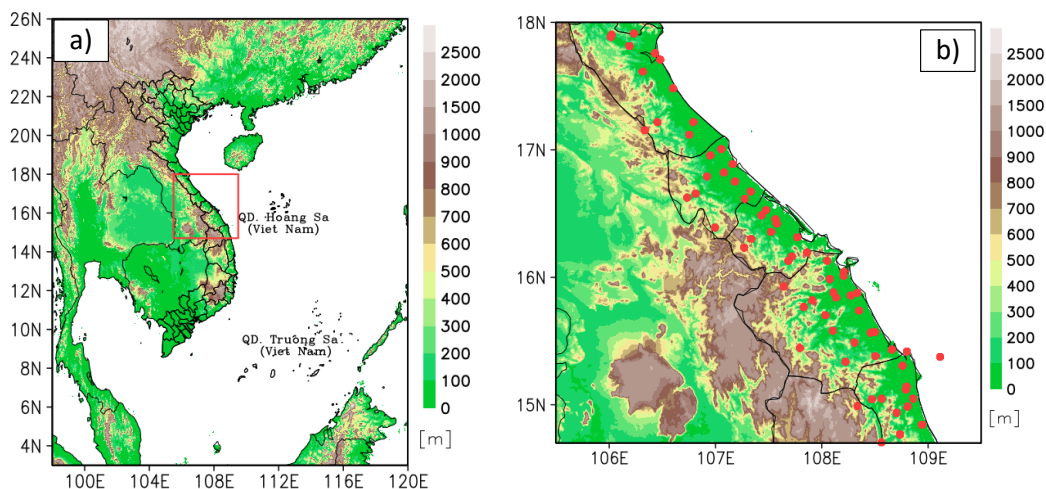
213 component. The lead time is 3 days, starting from 12:00 UTC 8 to 12:00 UTC 11 December
214 2018 with interval time of 6 hours. The horizontal resolution of this data is 6 km x 6 km.

215 2.2 Model description and experiment setup

216 We used the cloud-resolving model (CReSS). This model had been built and developed by
217 Nagoya University, Japan (Tsuboki and Sakakibara, 2002, 2007). This is a non-hydrostatic
218 and compressible cloud model, designed for simulation of various weather events at high
219 (cloud-resolving) resolution. In the model, the cloud microphysics is treated explicitly at
220 the user-selected degree of complexity, such as the bulk cold-rain scheme with six species:
221 vapor, cloud water, cloud ice, rain, snow, and graupel (Lin et al., 1983; Cotton et al., 1986;
222 Murakami, 1990, 1994; Ikawa and Saito, 1991). Other subgrid-scale processes
223 parameterized, such as turbulent mixing in the planetary boundary layer, as well as physical
224 options for surface processes, including momentum/energy fluxes, shortwave and
225 longwave radiation are summarized in Table 1.

226 To evaluate of the predictability of the D18 event using an ensemble time-lagged high-
227 resolution system and investigate the ensemble sensitivity of variables for the rainfall, 29
228 experiments were performed. The first members ran at 12:00 UTC on 3 December 2018,
229 and the last member ran at 12:00 UTC on 10 December 2018. Between the first and the
230 last members are multiple members running every 6-h (for a simulation length of 192 h).

231 All experiments using a single domain at 2.5 km horizontal grid spacing and a (x, y, z)
232 dimension of 912 x 900 x 60 grid points (Table 1, cf. Figure 2a). As introduced in
233 subsection 2.1.1, the NCEP GDAS/FNL Global Gridded Analyses and Forecasts (0.25° x
234 0.25°, every 6 h, 26 pressure levels) was used as the IC/BCs of the model.



235

236 **Figure 2.** (a) The simulation domain of the CReSS model and topography (m, shaded)
 237 used in the study. The red box marks the study area. (b) The distribution of the
 238 observation stations (red dots) in the study area.

239 Table 1. The basic information of experiments.

Domain and Basic setup	
Model domain	3°–26°N; 98°–120°E
Grid dimension (x, y, z)	912 × 900 × 60
Grid spacing (x, y, z)	2.5 km × 2.5 km × 0.5 km*
Projection	Mercator
IC/BCs (including SST)	NCEP GDAS/FNL Global Gridded Analyses and Forecasts (0.25° × 0.25°, every 6 h, 26 pressure levels)
Topography (for CTRL only)	Digital elevation model by JMA at (1/120)° spatial resolution



Simulation length	192 h
Output frequency	1 hour
Model physical setup	
Cloud microphysics	Bulk cold-rain scheme (six species)
PBL parameterization	1.5-order closure with prediction of turbulent kinetic energy (Deardorff, 1980; Tsuboki and Sakakibara, 2007)
Surface processes	Energy and momentum fluxes, shortwave and longwave radiation (Kondo, 1976; Louis et al., 1982; Segami et al., 1989)
Soil model	41 levels, every 5 cm deep to 2 m

240 * The vertical grid spacing (Δz) of CReSS is stretched (smallest at bottom) and the
241 averaged value is given in the parentheses

242 2.3 Verification of model rainfall

243 In order to verify the model-simulated rainfall, some verification methods are used,
244 including (1) visual comparison between the model and the observation (from the 69
245 automated gauges over the study area), and (2) the objective verification using categorical
246 skill scores at various rainfall thresholds from the lowest at 0.05 mm up to 900 mm for
247 three-day total. These scores are listed in Table 2 along with their formulas, perfect value,
248 and worst value, respectively. To apply these scores at a given threshold, the model and
249 observed value pairs at all verification points (gauge sites here, N) are first compared and
250 classified to construct a 2×2 contingency table (Wilks, 2006). At any given site, if the
251 event takes place (reaching the threshold) in both model and observation, the prediction is
252 considered a hit (H). If the event occurs only in observation but not the model, it is a miss
253 (M). If the event is predicted in the model but not observed, it is a false alarm (FA). Finally,



254 if both model and observation show no event, the outcome is correct rejection (*CR*). After
255 all the points are classified into the above four categories, the scores can be calculated by
256 their corresponding formula as:

257 Bias Score (*BS*) = $(H+FA)/(H+M)$, (1)

258 Probability of Detection (*POD*) = $H/(H+M)$, (2)

259 False Alarms Ratio (*FAR*) = $FA/(H+FA)$, (3)

260 Threat Score (*TS*) = $H/(H+M+FA)$, (4)

261 The values of *TS*, *POD*, and *FAR* are all ranged from 0 to 1, and the higher value is the
262 better for *TS* and *POD*, and conversely for *FAR*. For *BS*, its value can vary from 0 to $N-1$
263 and indicate the overestimation (underestimation) of the model for the events.

264 2.3.1 The Similarity Skill Score

265 In addition to the categorical scores, the Similarity Skill Score (*SSS*, Wang et al., 2022) is
266 also applied to evaluate the model rainfall results, as

267
$$SSS = 1 - \frac{\frac{1}{N} \sum_{i=1}^N (F_i - O_i)^2}{\frac{1}{N} \sum_{i=1}^N F_i^2 + \frac{1}{N} \sum_{i=1}^N O_i^2}$$
 (5)
268

269 where N is the total number of verification points, F_i is the forecast rainfall amount, and O_i
270 is the observed value, at the i th point among N , respectively. The *SSS* is a measure against
271 the worst mean squared error (*MSE*) possible. The formula shows that a forecast with
272 perfect skill has an *SSS* of 1, while a score of 0 means zero skill (model rainfall does not
273 overlap with the observation anywhere).

274 2.3.2. The ensemble spread (standard deviation)

275 The ensemble spread is considered a measure of the difference between the members to
276 the ensemble mean and known as the standard deviation (*SD*). In other words, the ensemble
277 spread will reflect the diversity of all possible outcomes. Hence, the ensemble spread is



278 often applied to predict the magnitude of the forecast error. If small spread indicates high
279 theoretical forecast accuracy, and large spread indicates low theoretical forecast accuracy.
280 Spread is computed by formulated below:

281

$$282 \quad SD = \sqrt{\frac{\sum_{i=1}^n (x_i - \mu_x)^2}{n-1}} \quad (6)$$

283 where x_i is the prediction value of member i , μ_x is the ensemble mean, n is the number of
284 ensemble members.

285 2.3.3. Ensemble Sensitivity Analysis

286 As mentioned above, an ensemble forecast is a set of forecasts produced by many separate
287 forecasts with differences in initial conditions, respectively. Moreover, as we know, the
288 numerical weather forecasts are sensitive to small changes in initial conditions and
289 sensitivity analysis is considered a measure to improve forecasts through targeting
290 observations. Hence, this study used the ESA method which is introduced by [Ansell and](#)
291 [Hakim \(2007\)](#) to examine how a forecast variable responds to changes in initial conditions.
292 The ensemble sensitivity is computed by the formula:

293

$$\frac{\partial R}{\partial x_t} = \frac{COV(R, x_t)}{var(x_t)} \quad (7)$$

294 Here, the response function R is chosen to be the areal-mean 24-h accumulated rainfall in
295 central Viet Nam (15.5°-16.3°N, 107.9°-108.6°E) on the rainiest day, from 12:00 UTC on
296 9 to 12:00 UTC on 10 December 2018. The starting time of this period, i.e., 12:00 UTC on
297 9 December, is defined as t_0 . Various scalar variables are considered for x_t , while those
298 from 48 h earlier (t_{-48} , or 12:00 UTC on 7 December) to the time of t_0 at 24-h intervals.
299 The COV is the covariance of R and x_t , and var is the variance of x_t , respectively.

300 As the analysis in part 1, the D18 event is caused by combined effectively between the
301 atmospheric disturbances at lower levels, such as cold surge, easterly wind, and
302 topography, ensemble-based sensitivity analysis (ESA) has been applied for variables at



303 surface, near-surface, and mid-tropospheric levels to assess the sensitivity of initial
304 conditions to the predictability of the rainy field. In order to facilitate the comparison
305 among the impacts of different variables, this study normalized ESA results by using the
306 standardized anomaly in the denominator and expressed as the change in R (in mm) in
307 response to an increase in x_t by one SD.

308 **3 Model results**

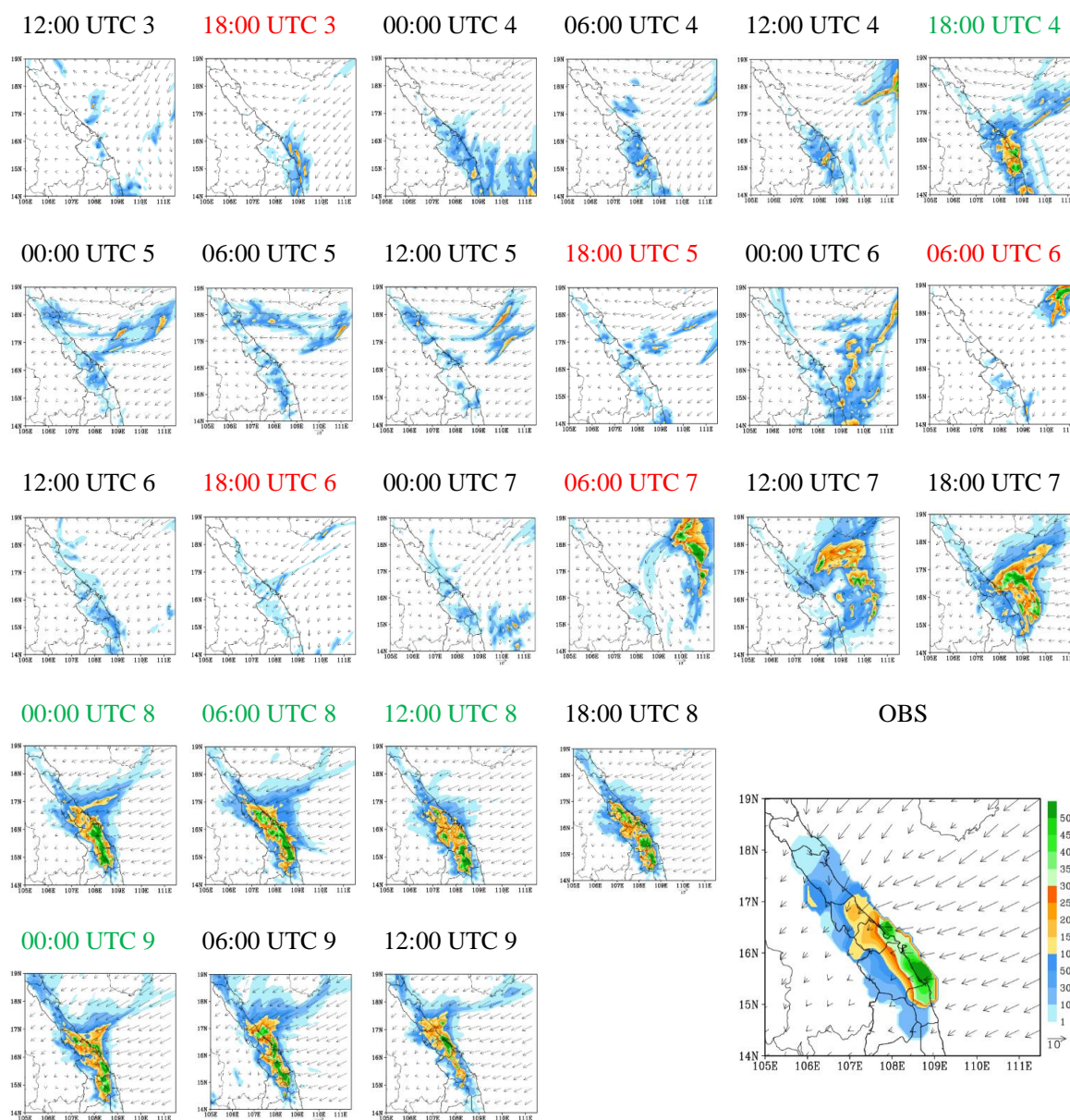
309 3.1 Time-lagged 24-h QPFs by the CReSS model

310 In this section, time-lagged forecasts targeted for the 24-h period from 12:00 UTC on 9 to
311 12:00 UTC on 10 December in the D18 event by the 2.5-km CReSS model are presented
312 and evaluated. This study focuses on this 24-h period because this is the rainiest day with
313 24-h observed data exceeding 600 mm at some stations (Fig. 3 OBS). Figure 3 shows 25
314 possible scenarios of 24-h rainfall and average surface winds over the target period
315 produced by the lagged runs every 6 h, with the earliest initial time at 12:00 UTC on 3
316 December and the latest one at 12:00 UTC on 9 December 2018, respectively. It is
317 immediately clear that several members made a rather good 24-h QPF not only in amounts,
318 but also in rainfall location and spatial distribution. These include most members executed
319 during 8-9 December, and also an impressive member that started at 18:00 UTC on 4
320 December. In this latter member, a reasonably good QPF was produced at a rather long
321 lead time, almost five days prior to the beginning of the target period (114 h). A common
322 feature among these good members is that they all captured the direction and magnitude of
323 surface winds quite well. On the other hand, most other members did poorly in their QPFs,
324 when executed before 06:00 UTC on 7 December at lead times beyond two days before
325 the target period. In general, they also could not predict the surface winds well enough.

326

327

328



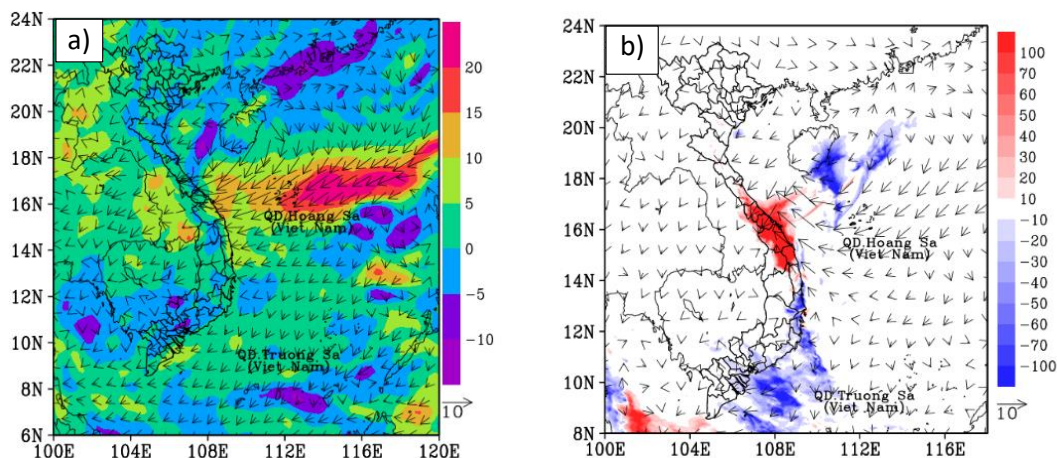
329 **Figure 3.** The predicted 24h accumulated rainfall (mm, shaded, scale on the right of panel
 330 OBS) and the mean surface horizontal wind (ms⁻¹, vector, reference length at panel OBS)
 331 on 10 December 2018 (from 12:00 UTC 9 December to 12:00 UTC 10 December 2018).
 332 The green color mark good members and the red color marks bad members. In OBS, 24h



333 observed rainfall (mm, shaded) and the surface wind derived from ERA5 data (ms^{-1} , vector),
334 adapted from Fig. 12f of Wang and Nguyen 2023.

335 The main reason for the significantly different forecast outcomes is elucidated in Fig. 4,
336 which depicts the mean differences in five good members (those with initial times at 18:00
337 UTC on 4, 00:00, 06:00, and 12:00 UTC on 8, and 00:00 UTC on 9 December) from five
338 bad ones (those ran at 18:00 UTC on 3, 18:00 UTC on 5, 06:00 and 18:00 UTC on 6, and
339 06:00 UTC on 7 December). In Fig. 4 (good minus bad members), it is clear that the surface
340 easterly winds were much stronger and the relative humidity much higher surrounding
341 central Viet Nam and its upstream areas in the GFS forecast data valid at 12:00 UTC on 9
342 December (used as BCs in CReSS runs) in the good members than in the bad ones. These
343 factors were identified as crucial for the extreme rainfall in the D18 event in Part 1, and
344 thus the good CReSS members produced much more rainfall in central Viet Nam (Fig. 4b).

345



346

347 **Figure 4.** The difference in (a) input data (boundary conditions) and (b) CReSS output
348 between averaged 5 good members (members ran at 18:00 UTC 4, 00:00 UTC 8, 06:00
349 UTC 8, 12:00 UTC 8, 00:00 UTC 9) and 5 bad members (members ran at 18:00 UTC 3,
350 18:00 UTC 5, 06:00 UTC 6, 18:00 UTC 6, 06:00 UTC 7). For input data, relative humidity



351 (% , shaded) and surface wind (ms^{-1} , vector) at 12:00 UTC December 9 2018. For CReSS
352 output, 24-h accumulated rainfall (mm, shaded) and surface wind (ms^{-1} , vector).

353 As we know, ensemble weather forecasts are a set of forecasts from multiple members that
354 represent the range of future weather possibilities, and the simplest way to use them is
355 through the ensemble mean (that emphasizes the features that the members agree upon). In
356 order to see how good CReSS can predict the D18 event with the time-lagged strategy,
357 from possible scenarios of 24 hours of rainfall of 10th December that produced by CReSS,
358 This study has grouped scenarios and computed them into different lead times using the
359 range of their initial times. It can be clearly seen in Fig. 5 that the rainfall produced by Fifth
360 4 and Sixth 4 members is quite similar to observed data, not only rainfall amount but also
361 the locations of significant rainbands and regions that concentrate mainly rainfall. For other
362 subgroup scenarios, the model made the rainfall scenarios much lower than observed
363 rainfall data. In which, third 4 and fourth 4 members are the lowest. It can be relevant to
364 the model that did not predict well the wind fields in every single running at extend ranges
365 (after day 3) as analyzed previous. The rainfall of second 4 members is the highest these
366 subgroup scenarios due to the model having single good-predict at 18:00 UTC on 4 [Fig.
367 3. (18:00 UTC 4)].

368

369

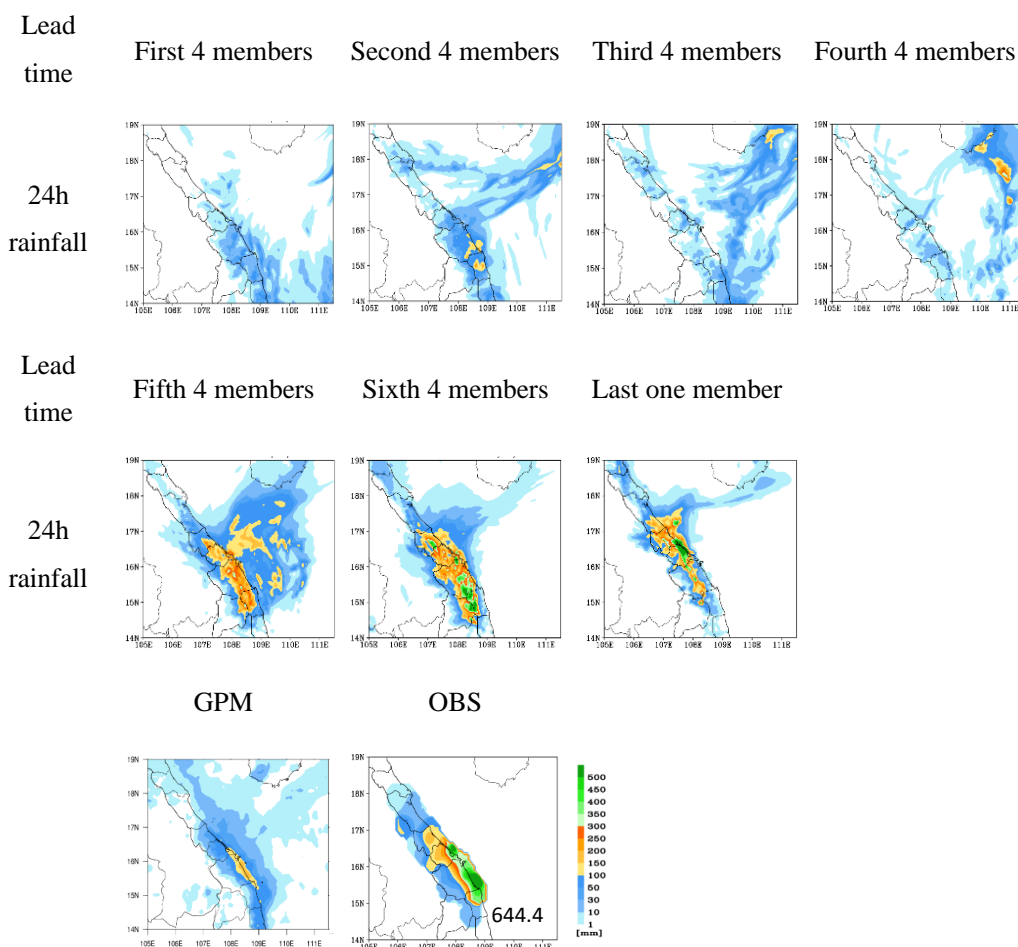
370

371

372

373

374



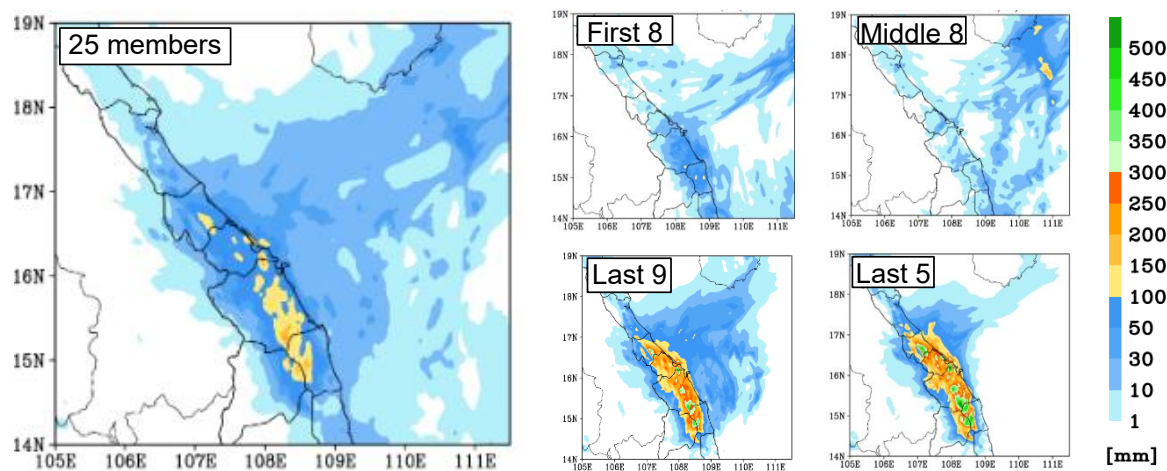
375 **Figure 5.** The predicted 24h rainfall by subgroup members, 24h accumulated rainfall by
376 the Global Precipitation Measurement (GPM) estimate (IMERG Final Run product), 24h
377 observed rainfall (mm, peak amount labeled at the lower-right corner) for the period of
378 12:00 UTC 9 December – 12:00 UTC 10 December 2018 as labelled. The same color bar
379 (lower right) is used for all panels.

380 Besides the evaluation on time-lagged results using batches of fixed number of successive
381 runs (every 4 members) as presented above, this study also grouped the members using
382 different ensemble sizes based on their behavior in order to better assess the temporal
383 evolution of forecast uncertainty and event predictability as the lead time shortened.



384 Particularly, this study divided the 25 members into several subgroups as shown in Fig. 6,
385 including the first eight members (those executed during 12:00 UTC 3 – 06:00 UTC 5
386 December), the middle eight members (run between 12:00 UTC 5 and 06:00 UTC 7
387 December), the last nine members (12:00 UTC 7–12:00 UTC 9 December), and the last
388 five members (12:00 UTC 8–12:00 UTC 9 December), respectively. In other words, the
389 last five members were those executed within 0-24 h (1 day) prior to the beginning of the
390 target period, and so on. In Fig. 6, it is clear that both the ensemble means from the last
391 five and the last nine members compare quite favorable to the observation, not only in the
392 accumulated amount but also in spatial distribution of rainfall. This indicates that the model
393 could produce QPFs at fairly good quality and rather consistently since the time as early as
394 roughly 48 h prior to the commencement of the rainfall event (also Fig. 3). These two sub-
395 ensemble groups within the short range gave much better quality in QPFs than the other
396 sub-groups executed before them at longer lead times, including the first eight, middle
397 eight, and all 25 members. In terms of skill scores, for example, the mean QPF by the last
398 five members have $TS = 0.4$, $POD = 0.8$, $FB = 1.5$, and $FAR = 0.5$ at 100 mm (per 24 h),
399 while the last nine members give similar scores of $TS = 0.5$, $POD = 0.8$, $FB = 1.4$, and
400 $FAR = 0.5$ (Figs. 7a-d), respectively. On the contrary, the mean QPFs from both the middle
401 eight and first eight members only yield zero scores in TS , POD , and FB with no skill in
402 FAR at 100 mm, obviously due to not enough rainfall in central Viet Nam in most of their
403 members. At 200 mm (per 24 h), similarly, the last five members ($TS = 0.2$, $POD = 0.4$,
404 $FB = 1.4$, and $FAR = 0.7$) and the last nine members ($TS = 0.3$, $POD = 0.5$, $FB = 1.2$, and
405 $FAR = 0.6$) again produce much better scores in QPFs, compared to no skill in all four
406 scores in QPFs from the middle eight, first eight, and all 25 members (Fig. 8a-d). In SSS,
407 the mean from the last nine members exhibits the highest score (0.64), the middle eight
408 members have the lowest score (0.04), and the mean from all 25 members is 0.43 (Fig. 7e).

409



410

411 **Figure 6.** Ensemble mean rainfall (shaded, scale on the right) from all 25 time-lagged
412 members, executed every 6 h from 12:00 UTC 3 December to 12:00 UTC 9 December, for
413 the 24h period from 12:00 UTC 9 December to 12:00 UTC 10 December.

414

415

416

417

418

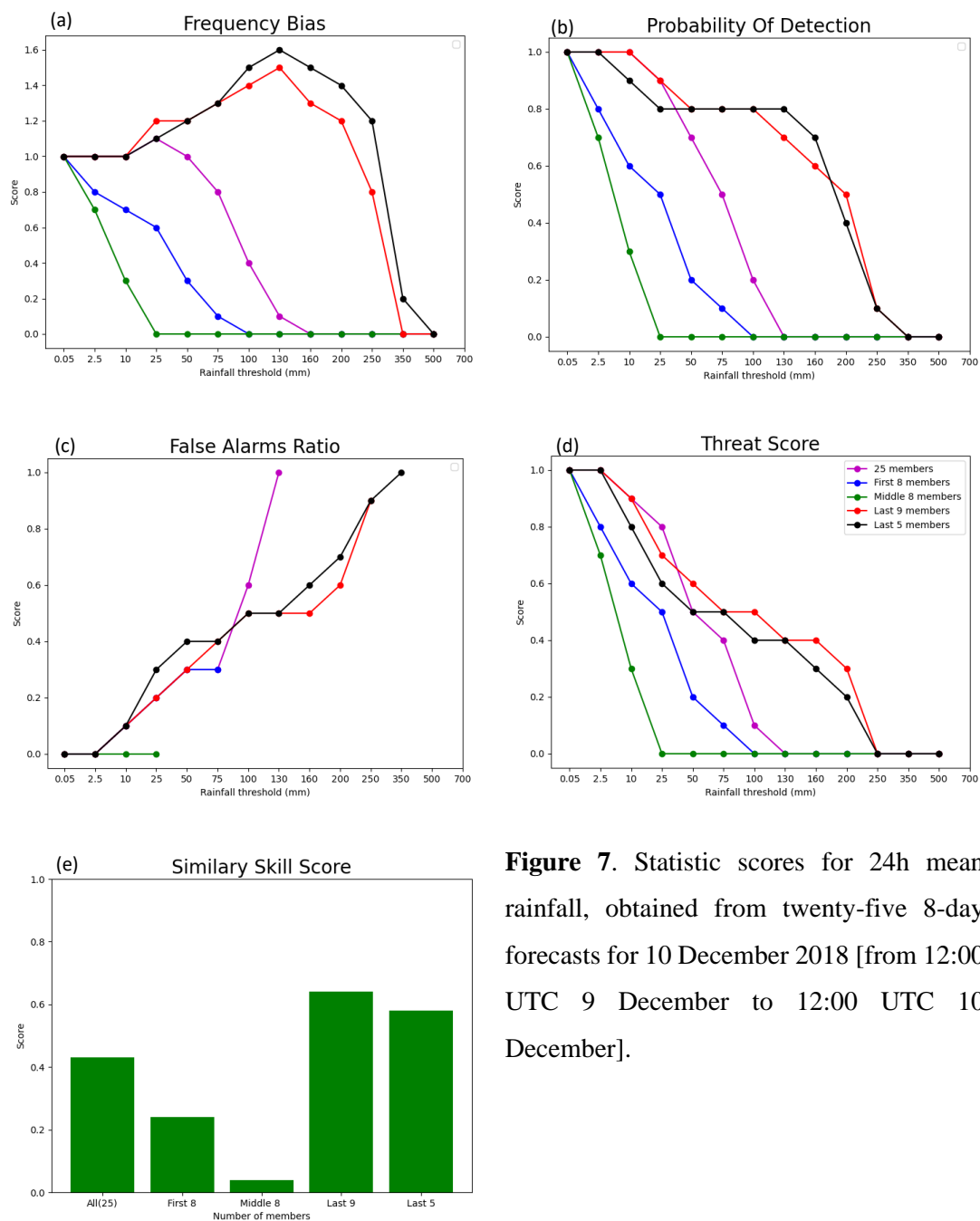
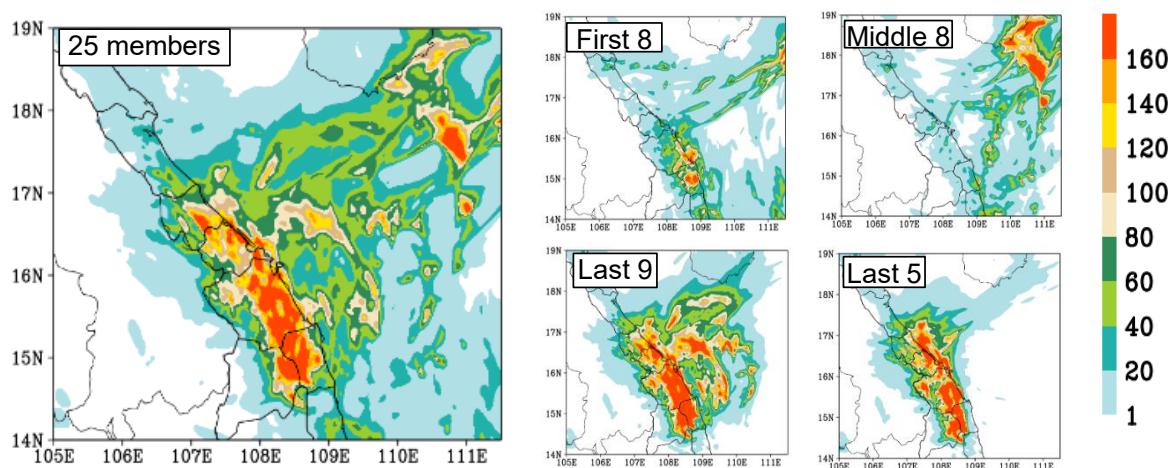


Figure 7. Statistic scores for 24h mean rainfall, obtained from twenty-five 8-day forecasts for 10 December 2018 [from 12:00 UTC 9 December to 12:00 UTC 10 December].



420 However, as indicated by the SD, the spreads in rainfall scenarios in both ensembles from
421 the last five and nine members are quite large (Fig. 8). Thus, while the lagged members
422 can produce a wide range of possible rainfall scenarios for the D18 event, which is the
423 main purpose of an ensemble as reviewed (Section 1), the members often cannot agree on
424 the precise locations of heavy rainfall. Given the small scale of local convection during the
425 event, this result is perhaps anticipated. On the other hand, the maxima in spread are >160
426 mm in Fig. 8 among the last nine members, and reasonable in magnitude compared to the
427 peak amounts of about 400 mm in the ensemble mean. In any case, Figs. 7 and 8 indicate
428 that the predictability of the D18 event changed considerably with time, and the 2.5-km
429 CReSS has a good skill in QPFs inside the short range (≤ 72 h). However, it is difficult to
430 predict the event successfully at longer lead times.



431
432 **Figure 8.** The spread (shaded, scale on the right) from all 25 time-lagged members,
433 executed every 6 h from 12:00 UTC 3 December to 12:00 UTC 9 December, for the 24h
434 period from 12:00 UTC 9 December to 12:00 UTC 10 December.

435 The probability information derived from the sub-ensemble groups at four different rainfall
436 thresholds from 100 to 450 mm is shown in Fig. 9, in which the increase in heavy-rainfall
437 probability in central Viet Nam and thus the predictability of the event with time is also



438 evident. From the first eight members executed at the longest range (≥ 102 h prior to rainfall
439 accumulation), there is only a 10-25% chance in parts of central Viet Nam to receive at
440 least 100 mm of rainfall (from 12:00 UTC 9 to 12:00 UTC 10 December). The probability
441 is even lower from the middle eight members (run between 54-96 h prior to target period),
442 as their SSS is the lowest among all sub-ensemble groups and only a couple of the runs
443 could reach 100 mm anywhere inland in central Viet Nam. As the lead time shortens to
444 inside the short range, the probabilities to have ≥ 100 mm of rainfall increase dramatically,
445 to roughly 70-80 % in the last nine members and further to over 80-90% in the last five
446 members. Due to the contribution from later members, about 20-40% of all 25 members
447 can reach 100 mm inland. Toward higher thresholds, the probabilities decrease in Fig. 9 as
448 expected, so are the areal sizes actually reaching those thresholds (red contours). At the
449 highest value of 450 mm, the ensembles in general show less than about 20% and 30%
450 chances for its occurrence from the last five and last nine members, respectively, and the
451 high probability areas are also slightly more inland than the observed one.

452

453

454

455

456

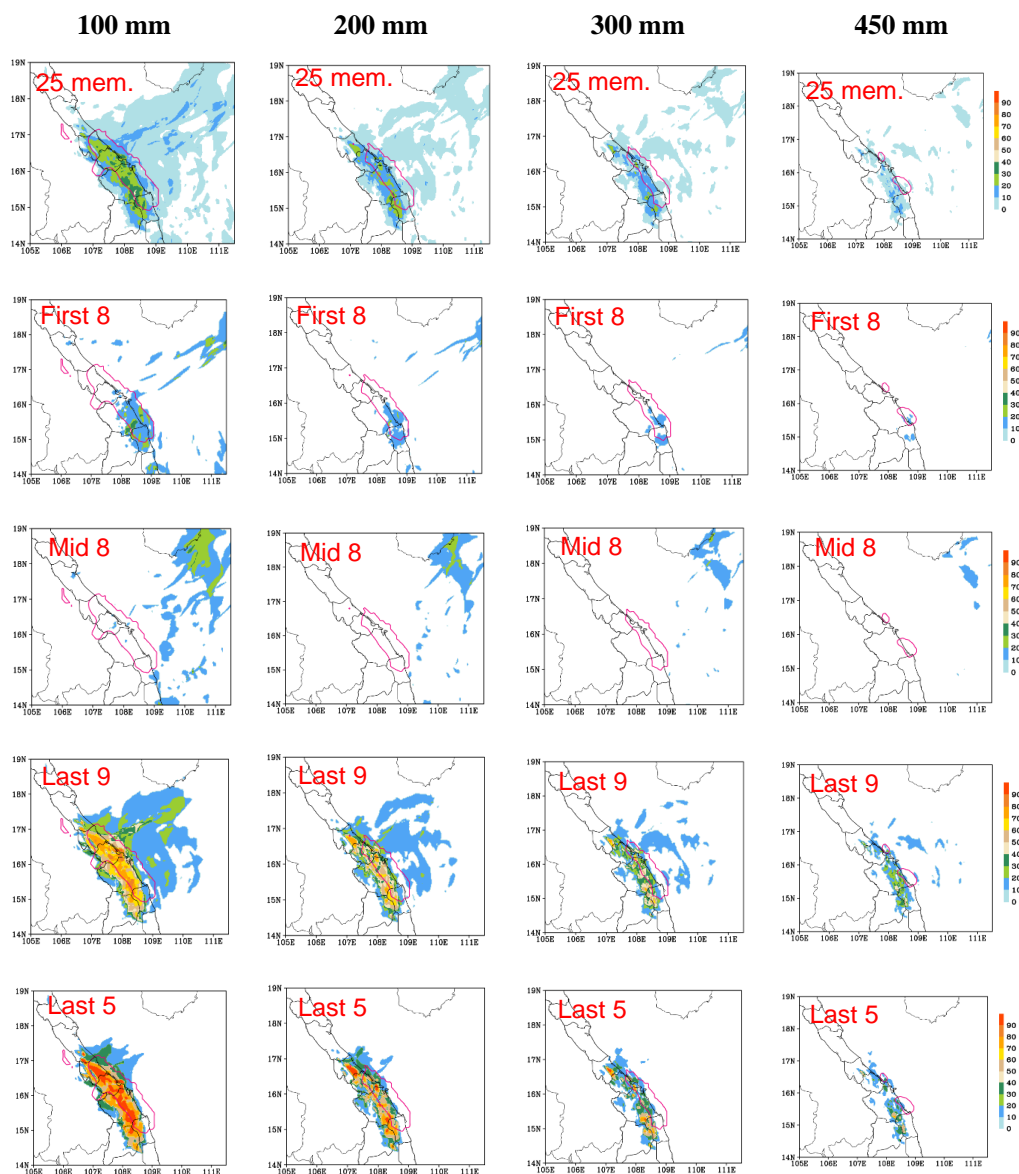
457

458

459

460

461



462 **Figure 9.** Probability distribution (%; shaded, scale on the right) from all 25 time-lagged
463 members, executed every 6 h from 12:00 UTC 3 December to 12:00 UTC 9 December,
464 reaching thresholds of 100, 200, 300, and 450 mm, for the 24h period from 12:00 UTC 9
465 December to 12:00 UTC 10 December. The observed areas at the same thresholds are



466 depicted by the pink contours. For each picture, red labeled at the top-left corner show the
467 number of members grouped to calculate the probability distribution.

468 3.2 Ensemble-based sensitivity analysis

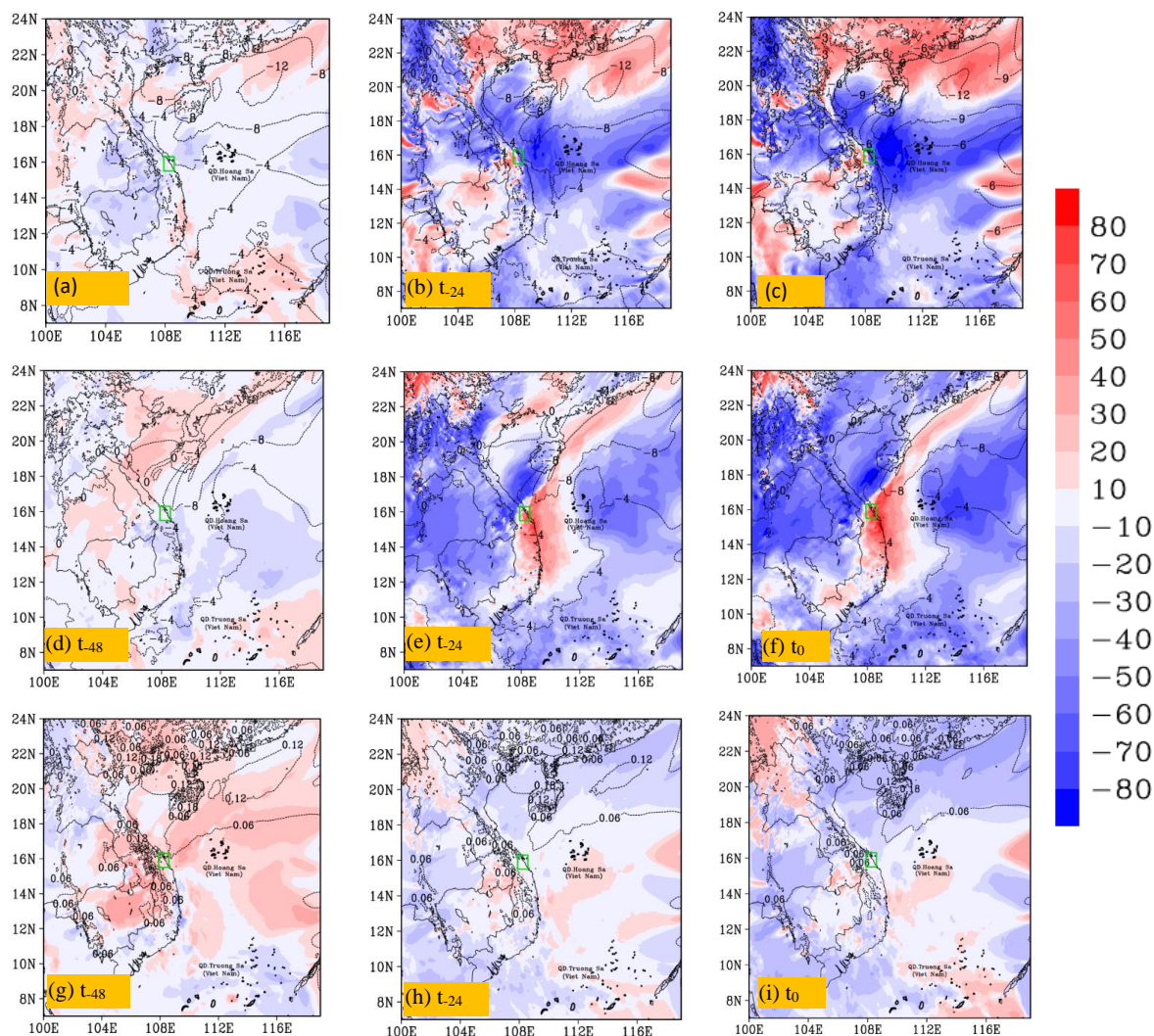
469 The results in part 3.1 above reveal that the CReSS model with a horizontal resolution of
470 2.5 km had well QPF predicted the rainiest day of the event while other models can't
471 capture it. Therefore, this part was made rely on this good performance. Figure 10 shows
472 the sensitivity of mean 24-h total rainfall inside the green box in central Viet Nam (R) to
473 zonal (u) and meridional (v) wind components and water vapor mixing ratio (q_v) at the
474 altitude of 100 meters, and the ensemble mean are also plotted. It is clear that the sensitivity
475 of rainfall to these variables is lower at longer forecast ranges and becomes higher at shorter
476 lead times. Specifically, from two days before (t_{-48}) to the starting time of the accumulation
477 period (t_0), the sensitivity of rainfall to u -wind over the SCS and along the coast of central
478 Viet Nam turned more negative, indicating heavier rainfall associated with stronger
479 easterly winds ($u < 0$) near the surface, especially in areas immediately upstream at t_0 . The
480 rainfall's sensitivity to v -wind leading to t_0 , on the other hand, exhibited a dipole structure,
481 with negative values to the north-northwest and positive values to the south-southeast
482 across central Viet Nam and the upstream ocean. This structure indicates a stronger
483 confluence in northeasterly winds over the region in rainier members, consistent with the
484 results in Part 1. In Figs. 10d-f, the increase in v -wind just south of central Viet Nam is
485 particularly evident, from -10 mm (per SD) at t_{-48} to over $+70$ mm (per SD) at t_0 . Thus, the
486 precipitation amount in the D18 event in central Viet Nam is highly sensitive to the
487 northeasterly winds in short range forecasts. In contrast, compared to the winds, the rainfall
488 was less sensitive to the water vapor amount as shown in Figs. 10g-i.

489

490

491

492



493

494 **Figure 10.** The sensitivity (mm, per SD, color, scale on the right) of areal-mean 24h
 495 accumulated rainfall in central Viet Nam starting from t_0 (i.e., R, averaging area depicted
 496 in green box) to surface wind components (ms^{-1} , shaded) and the ensemble mean (contours,
 497 every 4 ms^{-1}) and to surface water vapor mixing ratio (r , g kg^{-1}) and its ensemble mean
 498 (contours, every 0.06 g kg^{-1}) at different times at 24h intervals from (a) t_{-48} to (f) t_0 . The
 499 time of t_0 is 12:00 UTC 9 December 2018. In which, (a), (b), (c) for the zonal wind



500 component. (d), (e), (f) for the meridional wind component, and (g), (h), (i) for surface
501 water vapor mixing ratio.

502 Slightly higher at 1476 m (near 850 hPa), where easterly flow prevailed during the D18
503 event (see Fig. 3b in Part 1), the sensitivity of rainfall to winds exhibits similar spatial
504 patterns (Figs. 11a-f) to those at the altitude of 100 meters, with stronger easterly winds
505 and larger confluence in association with heavier rainfall. On the other hand, note that the
506 rainfall becomes more sensitive to mixing ratio in central Viet Nam at this level (Figs. 11g-
507 i), especially at shorter lead times, compared to its insensitivity to surface moisture amount.
508 Presumably, this positive correlation is due to upward transport of moisture, as the
509 ascending motion in convective clouds could become larger at this level.

510

511

512

513

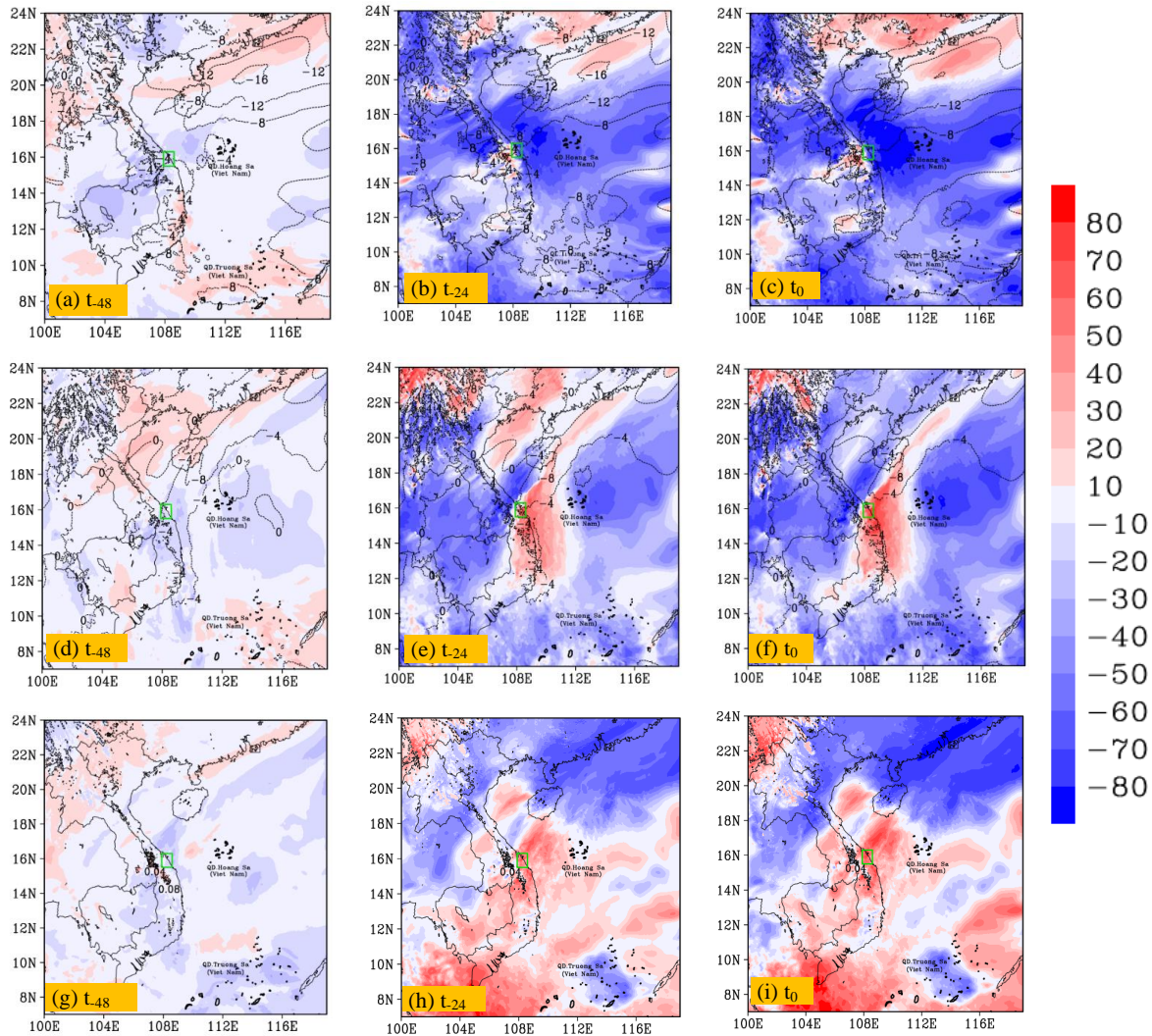
514

515

516

517

518



519

520 **Figure 11.** The sensitivity (mm, per SD, color, scale on the right) of 24h accumulated
 521 rainfall in central Viet Nam starting from t_0 (i.e., R, averaging area depicted in green box)
 522 to the wind components (ms^{-1} , shaded) and the ensemble mean (contours, every 4 ms^{-1})
 523 and to water vapor mixing ratio (r , g kg^{-1}) and its ensemble mean (contours, every 0.06 g
 524 kg^{-1}) at attitude of 1476 m and at different times at 24h intervals from (a) t_{-48} to (f) t_0 . The
 525 time of t_0 is 12:00 UTC 9 December 2018. In which, (a), (b), (c) for the zonal wind



526 component. (d), (e), (f) for the meridional wind component, and (g), (h), (i) for water vapor
527 mixing ratio.

528 At the upper level of 5424 m (near 500 hPa), it is seen that from t_{-48} to t_0 , dipole structures
529 developed in the sensitivity patterns to both u and v winds (Figs. 12a-f). To u winds,
530 positive sensitivity up to about +70 mm (per SD) existed to the south and negative
531 sensitivity up to -70 mm (per SD) to the north of central Viet Nam. Meanwhile, positive
532 sensitivity to v -wind appeared to the north and east with negative sensitivity to the south
533 and west of the rainfall area. While the prevailing winds at 500 hPa were southeasterly
534 over southern Viet Nam and southwesterly over northern Viet Nam during D18 (thus with
535 anticyclonic curvature, see Fig. 3c in Part 1), the above sensitivity patterns, apparent at t_{-24}
536 already, corresponded to stronger diffluence/divergence and a weaker anticyclone aloft to
537 favor more rainfall. To q_v , positive sensitivity signals up to +70 mm (per SD) also appeared
538 over the rainfall area at t_{-24} and t_0 (Figs. 12h,i), and the reason is similar to those near 850
539 hPa in Fig. 11.

540

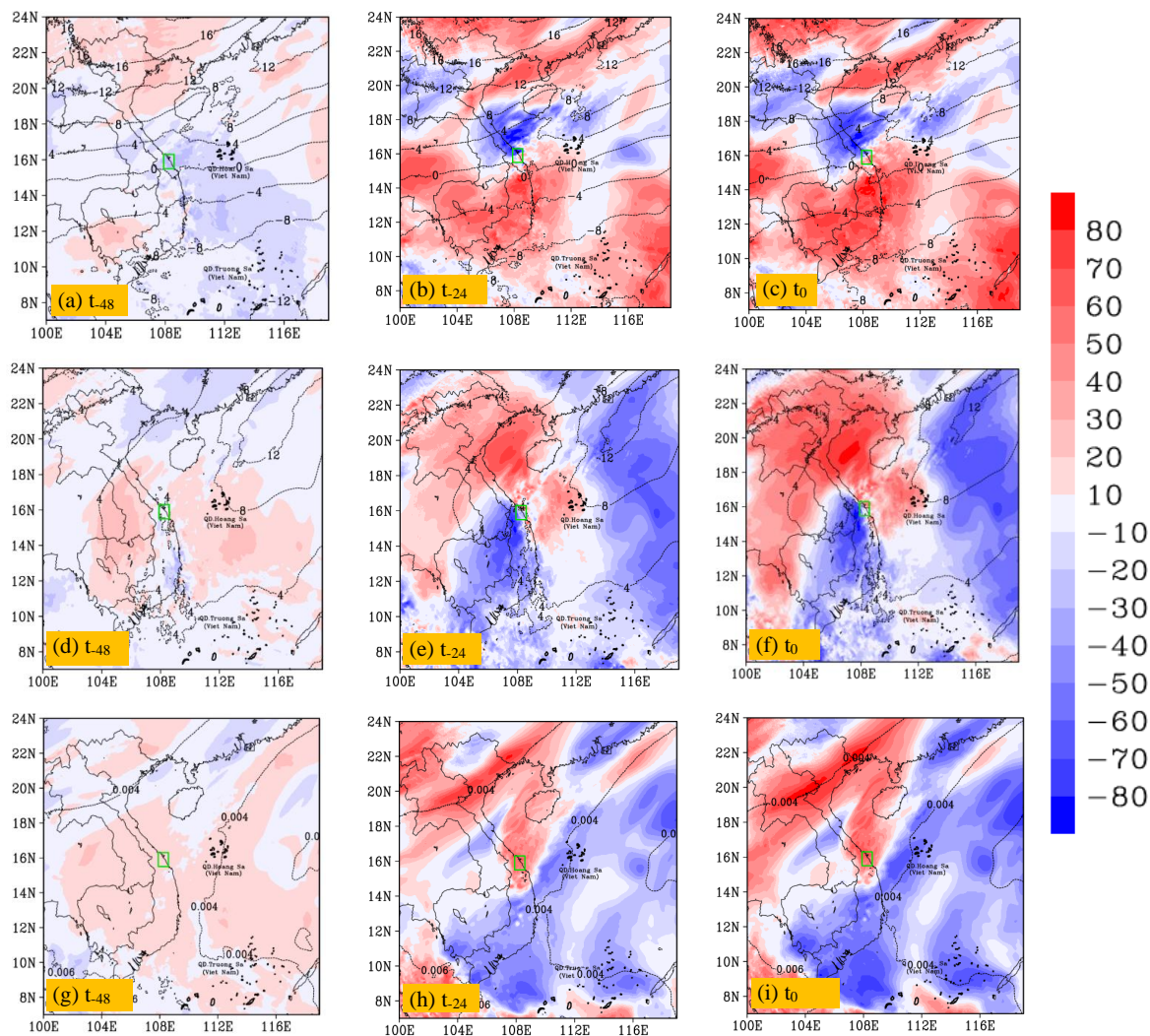
541

542

543

544

545



546 **Figure 12.** The sensitivity (mm, per SD, color, scale on the right) of 24h accumulated
 547 rainfall in central Viet Nam starting from t_0 (i.e., R, averaging area depicted in green box)
 548 to the wind components (ms^{-1} , shaded) and the ensemble mean (contours, every 4 ms^{-1})
 549 and to water vapor mixing ratio (r , g kg^{-1}) and its ensemble mean (contours, every 0.06 g
 550 kg^{-1}) at attitude of 5424 m and at different times at 24h intervals from (a) t_{-48} to (f) t_0 . The
 551 time of t_0 is 12:00 UTC 9 December 2018. In which, (a), (b), (c) for the zonal wind



552 component. (d), (e), (f) for the meridional wind component, and (g), (h), (i) for water
553 vapor mixing ratio.

554 4 Conclusion

555 As high resolution is required in numerical models to predict heavy rainfall more
556 successfully, the present work utilizes a time-lagged high-resolution ensemble forecast
557 system and evaluates how well the D18 event (during 9-12 December 2018) in central Viet
558 Nam can be predicted in advance before its occurrence. Using the CReSS model with a
559 grid size of 2.5 km (912×900 in dimension with 60 vertical levels), ensemble forecasts
560 were produced with a total of 29 time-lagged runs at 6-h intervals, each out to a forecast
561 range of 192 h (eight days). Our evaluation results in predictability indicate that the 2.5-
562 km system predicted the rainfall fields on 10 December during the event fairly well,
563 including both the amount and spatial distribution, within the short range at lead times of
564 day 1, 2, and 3. More specifically, the SSS of QPFs at these three ranges are about 0.4, 0.6,
565 and 0.7, respectively, with fairly consistent results among successive runs that indicate a
566 reasonable predictability, despite some spread and disagreement on the precise locations
567 of heavy rainfall. The above good results are due to the model's capability to better predict
568 the conditions in the lower troposphere such as the wind fields.

569 At lead times longer than three days, however, the predictability of the event is lowered
570 due to a higher level of forecast uncertainty, and the quality of QPFs drops with significant
571 under-prediction. Nevertheless, good QPFs are still possible occasionally. At lead time
572 beyond six days, it is challenging to achieve a good QPF at thresholds greater than 100 mm
573 even with a high-resolution model. This is presumably linked to the rapid evolution of
574 atmospheric conditions surrounding Viet Nam in a tropical environment. In the present
575 study, a CRM is applied to forecast extreme rainfall in central Viet Nam for the first time.
576 Although still with certain limitations, our results do indicate hope to predict such events
577 successfully beforehand, at least within the short range. Therefore, based on the present
578 work, more studies on the predictability of extreme rainfall in Viet Nam are recommended
579 in the near future.



580 The present study also performed an ensemble sensitivity analysis to identify the important
581 factors that influenced the 24-h rainfall amount in central Viet Nam in the D18 event. The
582 result shows that the rainfall is most sensitive to the wind conditions in the lower
583 troposphere leading to the event, with more rain associated with stronger northeasterly to
584 easterly winds and their confluence. In addition, the rainfall also shows some sensitivity to
585 the moisture amount and winds further aloft at the upper levels. In the ESA, the finer-scale
586 features (convection) are also seen to link to synoptic conditions in their background,
587 implying that it is meaningful to apply ESA to control the perturbations in initial fields.

588 *Acknowledgements:* This study was supported by the project “*Research on the application*
589 *of the Cloud-resolving model integrated with the regional numerical model to a 6-hour*
590 *accumulated quantitative precipitation forecast with 24-48 hours lead time for Mid-*
591 *Central Viet Nam*”, which is funded by the Ministry of Natural Resources and Environment
592 (MONRE) under grant no. TNMT.2023.06.07, and also by the National Science and
593 Technology Council (NSTC) of Taiwan under grants MOST 111-2111-M-003-005 and
594 MOST 111-2625-M-003-001.

595 *Code and data availability.* The CReSS model used in this study and its user’s guide are
596 available at the model website at [http://www.rain.hyarc.nagoya-](http://www.rain.hyarc.nagoya-u.ac.jp/~tsuboki/cress_html/src_cress/CReSS2223_users_guide_eng.pdf)
597 [u.ac.jp/~tsuboki/cress_html/src_cress/CReSS2223_users_guide_eng.pdf](http://www.rain.hyarc.nagoya-u.ac.jp/~tsuboki/cress_html/src_cress/CReSS2223_users_guide_eng.pdf) (last access: 6
598 July 2023; Tsuboki and Sakakibara, 2007). The TIGGE data and its information are
599 available at <https://confluence.ecmwf.int/display/TIGGE/TIGGE+archive>. The NCEP
600 GFS dataset and its description are available at <https://rda.ucar.edu/datasets/ds084.1/>.

601 *Author contributions.* **Duc Van Nguyen** prepared datasets, executed the model
602 experiments, performed the analysis, and prepared the first draft of the manuscript. **Chung-**
603 **Chieh Wang** also prepared the first draft and provided the funding, guidance and
604 suggestions during the study, and they participated in the revision of the manuscript. **Kien**
605 **Ba Truong** provided the funding and participated revising of the manuscript. **Thang Van**
606 **Vu, Pham Thi Thanh Nga, and Pi-Yu Chuang** also participated in the revision of the
607 manuscript.



608 *Competing interests.* The authors declare that they have no conflict of interest.

609 **References**

610 Ancell, and Hakim, G. J.: Comparing adjoint- and ensemble sensitivity analysis with
611 applications to observation targeting. *Mon. Wea. Rev.*, 135, 4117–4134,
612 doi:10.1175/2007MWR1904.1, 2007.

613 Cotton, W. R., Tripoli, G. J., Rauber, R. M., and Mulvihill, E. A.: Numerical simulation of
614 the effects of varying ice crystal nucleation rates and aggregation processes on
615 orographic snowfall. *J. Appl. Meteorol. Clim.*, 25, 1658–1680, 1986.

616 Coleman, A. A., and Ancell, B. C.: Toward the improvement of high-impact probabilistic
617 forecasts with a sensitivity-based convective-scale ensemble subsetting
618 technique. *Mon. Wea. Rev.*, 148, 4995–5014, [https://doi.org/10.1175/MWRD-20-](https://doi.org/10.1175/MWRD-20-0043.1)
619 [0043.1](https://doi.org/10.1175/MWRD-20-0043.1), 2020.

620 Deardorff, J. W.: Stratocumulus-capped mixed layers derived from a three-dimensional
621 model. *Bound.-Lay. Meteorol.*, 18, 495–527, 1980.

622 Hu, C.-C., and Wu, C.-C.: Ensemble sensitivity analysis of tropical cyclone
623 intensification rate during the development stage. *J. Atmos. Sci.*, 77, 3387–
624 3405, <https://doi.org/10.1175/JAS-D-19-0196.1>, 2020.

625 Hoa, V. V.: Comparative study skills rain forecast the middle part and central highland of
626 several global models (In Viet Nameese). *Viet Nam journal of Hydrometeorology*. V.
627 667 No. 07 (2016), 2016.

628 Ikawa, M. and Saito, K.: Description of a non-hydrostatic model developed at the Forecast
629 Research Department of the MRI, MRI Technical report 28, Japan Meteorological
630 Agency, Tsukuba, Japan, ISSN: 0386-4049, 1991.

631 Kerr, C. A., Stensrud, D. J. and Wang, X.: Diagnosing convective dependencies on near-
632 storm environments using ensemble sensitivity analyses. *Mon. Wea. Rev.*, 147, 495–
633 517, <https://doi.org/10.1175/MWRD-18-0140.1>, 2019.



- 634 Kondo, J.: Heat balance of the China Sea during the air mass transformation experiment.
635 J. Meteorol. Soc. Jpn., 54, 382–398, https://doi.org/10.2151/jmsj1965.54.6_382, 1976.
- 636 Leith, C. E.: Theoretical skill of Monte Carlo forecasts. Mon. Wea. Rev., 102, 409–
637 418, 1974.
- 638 Lin, Y.-L., Farley, R. D., and Orville, H. D.: Bulk parameterization of the snow field in a
639 cloud model. J. Appl. Meteorol. Clim., 22, 1065–1092, 1983.
- 640 Louis, J. F., Tiedtke, M., and Geleyn, J. F.: A short history of the operational PBL
641 parameterization at ECMWF, in: Proceedings of Workshop on Planetary Boundary
642 Layer Parameterization, 25–27 November 1981, Shinfield Park, Reading, UK, 59–79,
643 1982.
- 644 Murphy, J. M.: The impact of ensemble forecasts on predictability. Quart. J. Roy.
645 Meteor. Soc., 114, 463–493, 1988.
- 646 Murakami, M.: Numerical modeling of dynamical and microphysical evolution of an
647 isolated convective cloud – the 19 July 1981 CCOPE cloud. J. Meteorol. Soc. Jpn., 68,
648 107–128, 1990.
- 649 Murakami, M., Clark, T. L., and Hall, W. D.: Numerical simulations of convective snow
650 clouds over the Sea of Japan: Two dimensional simulation of mixed layer development
651 and convective snow cloud formation. J. Meteorol. Soc. Jpn. 72, 43–62, 1994.
- 652 Nhu, D. H., Anh, N. X., Phong, N. B., Quang, N. D., and Hiep, V. N.: The role of
653 orographic effects on occurrence of the heavy rainfall event over central Viet Nam in
654 November 1999. Journal of Marine Science and Technology. V. 17, No. 4B(2017), 31–
655 36, 2017.
- 656 Segami, A., Kurihara, K., Nakamura, H., Ueno, M., Takano, I., and Tatsumi, Y.:
657 Operational mesoscale weather prediction with Japan Spectral Model. J. Meteorol.
658 Soc. Jpn., 67, 907–924, https://doi.org/10.2151/jmsj1965.67.5_907, 1989.



- 659 Surcel, M., Zawadzki, I., and Yau, M. K.: On the filtering properties of ensemble
660 averaging for storm-scale precipitation forecasts. *Mon. Wea. Rev.*, 142, 1093–1105,
661 doi:10.1175/MWR-D-13-00134.1, 2014.
- 662 Son, B. M. and Tan, P. V.: Experiments of heavy rainfall prediction over South of Central
663 Viet Nam using MM5 (In Vietnamese). *Viet Nam Journal of Hydrometeorology.*,
664 4(580), 9–18, 2009.
- 665 Toan, T. N., Thanh, C., Phuong, P. T., and Anh, T. V.: Assessing the predictability of WRF
666 model for heavy rain by cold air associated with the easterly wind at high-level patterns
667 over mid-central Viet Nam (In Vietnamese). *VNU Journal of Science: Earth and
668 Environmental Sciences.* v. 34, n. 1S, dec. 2018. ISSN 2588-1094.
669 <https://js.vnu.edu.vn/EES/article/view/4328>, 2018.
- 670 Torn, R.D., Hakim, G.J.: Initial condition sensitivity of western Pacific
671 extratropical transitions determined using ensemble-based sensitivity analysis. *Mon.
672 Weather Rev.* 137, 3388–3406. <https://doi.org/10.1175/2009MWR2879.1>, 2009.
- 673 Tsuboki, K. and Sakakibara, A.: Numerical Prediction of HighImpact Weather Systems:
674 The Textbook for the Seventeenth IHP Training Course in 2007, Hydrospheric
675 Atmospheric Research Center, Nagoya University, Nagoya, Japan, and UNESCO,
676 Paris, France, 273 pp., [http://www.rain.hyarc.nagoya-u.ac.jp/~tsuboki/
677 cress_html/src_cress/CRess2223_users_guide_eng.pdf](http://www.rain.hyarc.nagoya-u.ac.jp/~tsuboki/cress_html/src_cress/CRess2223_users_guide_eng.pdf) (last access: 1 May 2019),
678 2007.
- 679 Wang, C.-C.*, Kuo, H.-C., Yeh, T.-C., Chung, C.-H., Chen, Y.-H., Huang, S.-Y.,
680 Wang, Y.-W., and Liu, C.-H.: High-resolution quantitative precipitation forecasts and
681 simulations by the Cloud-Resolving Storm Simulator (CRess) for Typhoon Morakot
682 (2009). *J.Hydrol.*, 506, 26-41, <http://dx.doi.org/10.1016/j.jhydrol.2013.02.018>, 2013.
- 683 Wang, C.-C.*, Lin, B.-X., Chen, C.-T., and Lo, S.-H.: Quantifying the effects of long-term
684 climate change on tropical cyclone rainfall using cloud-resolving models:
685 Examples of two landfall typhoons in Taiwan. *J. Climate*, 2015.



- 686 Wang, C.-C.: On the calculation and correction of equitable threat score for model
687 quantitative precipitation forecasts for small verification areas: The example of
688 Taiwan. *Wea. Forecasting*, 29, 788–798, doi:10.1175/WAF-D-13-00087.1, 2014.
- 689 Wang, C.-C., Huang, S.-Y., Chen, S.-H., Chang, C.-S., and Tsuboki, K.: Cloud resolving
690 typhoon rainfall ensemble forecasts for Taiwan with large domain and
691 extended range through time-lagged approach. *Wea. Forecasting*, 31, 151–172,
692 doi:10.1175/WAF-D-15-0045.1, 2016.
- 693 Wang, C.-C., Li, M.-S., Chang, C.-S., Chuang, P.-Y., Chen, S.-H., and Tsuboki, K.:
694 Ensemble-based sensitivity analysis and predictability of an extreme rainfall event
695 over northern Taiwan in the Mei-yu season: The 2 June 2017 case. *Atmos. Res.*, 259,
696 105684, <https://doi.org/10.1016/j.atmosres.2021.105684>, 2021.
- 697 Wang, C.-C., Tsai, C.-H., Jou, B. J.-D., and David, S. J.: Time-Lagged Ensemble
698 Quantitative Precipitation Forecasts for Three Landfalling Typhoons in the Philippines
699 Using the CReSS Model, Part I: Description and Verification against Rain-Gauge
700 Observations. *Atmosphere*, 13, 1193, <https://doi.org/10.3390/atmos13081193>, 2022.
- 701 Wang, C.-C., and Nguyen, D. V.: Investigation of an extreme rainfall event during 8–12
702 December 2018 over central Viet Nam – Part 1: Analysis and cloud-resolving
703 simulation. *Nat. Hazards Earth Syst. Sci.*, 23, 771–788, [https://doi.org/10.5194/nhess-](https://doi.org/10.5194/nhess-23-771-2023)
704 [23-771-2023](https://doi.org/10.5194/nhess-23-771-2023), 2023.
- 705 Wang, C.-C., Chen, S.-H., Chen, Y.-H., Kuo, H.-C., Ruppert, Jr., J. H., and Tsuboki, K.:
706 Cloud-resolving time-lagged rainfall ensemble forecasts for typhoons in Taiwan:
707 Examples of Saola (2012), Soulik (2013), and Soudelor (2015). *Wea. Clim. Extremes*,
708 40, 100555, <https://doi.org/10.1016/j.wace.2023.100555>, 2023.
- 709 Wilks, D. S.: *Statistical Methods in the Atmospheric Sciences*. Academic Press, 648 pp.,
710 ISBN 13: 978-0-12-751966-1, 10: 0-12- 751966-1, 2006.
- 711